Research Article

CT and MRI Evaluation of Nasal Adenocarcinoma Local Extent

Patrice GALLET[1,2*], Philippe HENROT[2,3], Bruno GRIGNON[2,3], Phi Linh NGUYEN THI[2,4], Roger JANKOWSKI[1,2]

1. Service ORL, Institut Louis Mathieu, CHRU Nancy, Rue du Morvan, 54000 Nancy, France
2. Université de Lorraine, Faculté de médecine, 9 Avenue de la Forêt de Haye, 54000 Nancy, France
3. Imagerie Guilloz, Hôpital Central, CHRU Nancy, 29 Bd du Marechal de Lattre de Tassigny, 54000 Nancy, France.
4. CIE6 Inserm: Service d'épidémiologie et évaluation cliniques, CHRU Nancy, Rue du Morvan, 54000 Nancy, France.

Abstract:

BACKGROUND AND PURPOSE: The radiological evaluation of the local extent of nasal adenocarcinomas may be complex. Objectives of this study were to describe the local extent of adenocarcinomas of the olfactory cleft relatively to the natural barriers of the sino-nasal cavities and to assess the reproducibility of this evaluation.

METHODS: We retrospectively analysed a 5-year series of pre-op CT and MRI images of patients operated on nasal adenocarcinoma. The tumoral extensions were staged according to their relationships with the surrounding anatomical barriers (from d1=at distance from the barriers to d4b=invasion of the adjacent organ with resectability impossible or uncertain) by two teams (each composed of one ENT and one radiologist), who blindly analysed the radiological records twice, using a standardized grid. Reproducibility was evaluated with the kappa test.

RESULTS: 30 radiological records were analysed. Results support that the origin of woodworkers' adenocarcinomas is in the olfactory cleft. Reproducibility was excellent for all the criteria (K=0.8) except for the relation with sphenoid sinus (K=0.5).

CONCLUSIONS: This study proposes to stage, in a precise and reproducible manner, the local extension of nasal adenocarcinomas according to their relationships with the surrounding barriers of the olfactory-ethmoidal cavities. This method of staging may help for rationalized therapeutic decision.

Keywords: nasal adenocarcinoma, woodworkers, ethmoid, reproducibility

Introduction

Nasal adenocarcinomas (ADC) are rare tumors, mostly consecutive to prolonged wood dust exposition. ADC usually originate in the olfactory cleft and present as a polyp like neoplasm, with a pedicle of variable size developed on one ore more walls of the olfactory cleft (1). The size of the pedicle is independent of tumoral volume. Endoscopic findings (1) and CT-scans analysis (2) suggest that ADC do not have a very aggressive behaviour, which is reflected in their low metastatic potential, and their local development that respects for long the surrounding structures. As a result, tumoral growth seems highly limited by the encountered barriers.

Craniofacial resection was for long the gold standard treatment, but endoscopic endonasal surgery has proven efficient in most situations (3,4). Indeed, the main goal of the surgical resection of the tumor is to perform the resection of the olfactory cleft, thus resecting the tumoral pedicle enclosed in its muco-periosteal sheath of olfactory cleft(4).

[*]**Corresponding author**: Patrice GALLET, Service ORL, Institut Louis Mathieu, CHRU Nancy, Rue du Morvan, 54000 NANCY, France. Phone number : +33383155419. Fax: +33383155421. Email: patrice.gallet@yahoo.fr
Citation: GALLET P, et al. CT and MRI evaluation of nasal adenocarcinoma local extent. Cancer Research Frontiers. 2015 Apr; 1(2): 191-199. doi: 10.17980/2015.191

Competing Interests: The authors declare that they have no competing interests.
Received December 30, 2014; Revised March 18, 2015; Accepted March 30, 2015.

However, intracranial extension is not impossible (10% in a multicentric GETTEC study (5)) and intraorbital extension may sometimes require orbital exenteration. Finally, some areas are of difficult access for endoscopic surgery, like the anterointerne angle of the orbit (behind the frontal process of the maxillar). It is therefore critical to precisely determine preoperatively the tumoral extension in relation to natural barriers of the nasal fossa. These anatomical barriers that a tumor originating in the olfactory cleft may respect or modify are the followings (6) (fig 1):

- Superiorly: the ethmoidal roof, which is actually composed of two distinct portions from within outwards the cribriform plate and the roof of the lateral mass of the ethmoid; the latter is divided into a vertical portion (the lateral lamella of the olfactory groove) and a horizontal portion (the ethmoidal roof, properly speaking).

- Laterally: the turbinate wall of the ethmoid, then the medial wall of the orbit, which is hinged forward with the frontal process of the maxilla and backward with the anterior and lateral faces of the sphenoid

- Posteriorly: the anterior wall of the sphenoid

- Medially: the nasal septum

The aim of this study was to describe the local extent of ADC in relation to these anatomical landmarks, and to assess the reproducibility of this evaluation.

Methods

We designed a retrospective, blind and randomized study to analyse the pre-op CT and MRI images of patients operated on olfactory cleft adenocarcinoma in order to test the intra and inter-observer reproducibility of a radiological reading grid developed with the aim to describe the relationships of the tumor with known anatomical barriers.

1. Construction of the radiological grid

The grid we used to describe the radiological relationships that a tumor of the olfactory cleft can develop with each of the five main landmarks was as follow:

- d1: the tumor stayed at distance from the landmark

- d2: the tumor came in contact with the landmark

- d3: the tumor lysed the bone of the landmark
  d3a: without any imprint onto the adjacent organ
  d3b: with an imprint onto the adjacent organ

- d4: the tumor was invading the adjacent organ
  d4a: the tumor seemed resectable
  d4b: the resectability of the tumor was uncertain or impossible (huge invasion of the brain or of the posterior part of the orbital content)

For the differentiation between d3b and d4a stages, we used the criteria developed by Eisen and Kraus (7–9), which are presented in the discussion.

2. Intra and inter-observer reproducibility

Two independent teams, each composed of one senior radiologist and one ENT, had to read the anonymized CT/MRI images of each case two times, with a minimal three-week interval.

2.1. Selection of patient records

The records of all patients operated on a nasal adenocarcinoma in our centre between May 1st 2004 and April 31th 2009 were included in the study, if both the pre-op CT and MRI images could be retrieved. Patients with incomplete radiological records (without axial or coronal series for MRI, with less than 30 frames in CT-axial series or without possibilities of coronal reconstructions) were excluded from the study, as patients with a history of previous sinus surgery.

2.2. Anonymisation and randomization of files

Any indication that could lead to the identification of patients (name, date of birth or examination, place of examination) was deleted on images. Radiological records were randomized with a random 8-digit number.

2.3. Reading process

The images were analysed in the conditions of usual clinical practice, on a console Agfa-Impax DS3000, displaying both the scanner and MRI.

2.4. Statistical analysis

Inter and intra-observer reliability was assessed by concordance analysis with the Kappa test (10). The ponderation was linear for variables with several categories. The inter-observer reproducibility was calculated only if the intra-observer reproducibility was superior to 0.4 in the two groups. The inter-observer reproducibility was calculated from the results of the second reading. The match was interpreted according to the criteria of Landis and Koch(11): excellent when Kappa was superior to 0.8, good between 0.61 and 0.8, moderate between 0.41 and 0.6, low between 0.21 and 0.4, negligible between 0 and 0.2. SAS 9.2 was used for the analysis.

Table 1: Intra and inter-observer reproducibility of the criteria

	Team-1			Team-2			Interjudge
	Reading-1 (n)	Reading-2 (n)		Reading-1 (n)	Reading-2 (n)		
Cribriform plate	**Intrajudge reproducibility**			**Intrajudge reproducibility**			**Interjudge reproducibility**
	K=0.7 ci(0.6-0.9)			**K=0.8** ci(0.6-1)			**K=0.8 ci(0.7-1)**
	d1	1	2	**d1**	3	1	**(K=0.7)**
	d2	21	19	**d2**	18	20	**(K=0.8)**
	d3a	.	3	**d3a**	4	4	**(K=0.3)**
	d3b	7	3	**d3b**	4	4	**(K=0.5)**
	d4a	1	3	**d4a**	1	1	**(K=0.5)**
	d4b	.	.	**d4b**	.	.	**ns**
Ethmoidal roof	**Intrajudge reproducibility**			**Intrajudge reproducibility**			**Interjudge reproducibility**
	K=0.8 ci(0.6-1)			**K=0.8** ci(0.7-1)			**K=0.8 ci(0.6-1)**
	d1	24	25	**d1**	21	23	**(K=0.8)**
	d2	.	1	**d2**	3	1	**ns**
	d3a	1	.	**d3a**	2	3	**ns**
	d3b	4	2	**d3b**	3	2	**(K=0.7)**
	d4a	1	2	**d4a**	1	1	**ns**
	d4b	.	.	**d4b**	.	.	**ns**
Orbital wall	**Intrajudge reproducibility**			**Intrajudge reproducibility**			**Interjudge reproducibility**
	K=0.9 ci(0.9-1)			**K=0.8** ci(0.7-1)			**K=0.8 ci(0.6-1)**
	d1	16	16	**d1**	15	15	**(K=0.8)**
	d2	3	4	**d2**	3	3	**ns**
	d3a	2	1	**d3a**	1	2	**(K=0.7)**
	d3b	8	9	**d3b**	9	9	**(K=0.8)**
	d4a	1	.	**d4a**	1	1	**ns**
	d4b	.	.	**d4b**	1	.	**ns**
Anterior sphenoid wall	**Intrajudge reproducibility**			**Intrajudge reproducibility**			**Interjudge reproducibility**
	K=0.5 ci(0.3-0.7)			**K=0.7** ci(0.5-0.9)			**K=0.5 ci(0.3-0.7)**
	d1	5	3	**d1**	4	3	**(K=0.3)**
	d2	14	16	**d2**	12	14	**(K=0.7)**
	d3a	5	1	**d3a**	9	9	**(K=0.5)**
	d3b	5	8	**d3b**	2	1	**(K=0.2)**
	d4a	1	2	**d4a**	3	3	**(K=0.8)**
	d4b	.	.	**d4b**	.	.	**ns**
Septum	**Intrajudge reproducibility**			**Intrajudge reproducibility**			**Interjudge reproducibility**
	K=0.7 ci(0.6-0.9)			**K=0.8** ci(0.6-1)			**K=0.8 ci(0.7-1)**
	d1	.	.	**d1**	.	.	**ns**
	d2	2	2	**d2**	2	2	**(K=1)**
	d3a	.	.	**d3a**	.	.	**ns**
	d3b	15	18	**d3b**	22	21	**(K=0.8)**
	d4a	13	10	**d4a**	8	9	**(K=0.6)**
	d4b	.	.	**d4b**	.	.	**ns**

ns: kappa values are not statistically significant

Results

1. Study population

During the five-year period of the study, forty-two patients in total were operated for nasal adenocarcinoma, of which eleven were excluded because pre-op images were not available anymore. One patient was excluded because of a history of previous ethmoid surgery.

Of the 30 patients finally included in the study, only 12 had been classified according to the TNM UICC-2002 classification, regarding the local extension (1 T1, 5 T2, 3 T3, 3 T4b). The pedicle of the tumor could endoscopically be detected in the olfactory cleft in 27/30 patients.

2. Quality of the study imaging material

Radiological exams were performed in different centres, with variable scanning and MRI parameters. Slide thickness was submillimetric in 25 cases (83.3%). Dental artifacts were present in 10 cases (33.3%), but were generally not troublesome as they did not concern the studied barriers. MRI series at our disposal usually included 8 to 10 different sequences, which always enabled analysis. Though 8 MRI were lacking T1 without injection axial sequences and 9 were performed without T2 frontal sequences.

3. Descriptive analysis and reproducibility (table 1)

All tumors could be classified according to the radiological grid. The intra-observer reproducibility was superior to 0.4 for all criteria. For easier understanding of the data, we report in this section only the inter-observer reproducibility, unless otherwise specified.

3.1. Relationship with the cribriform plate

The reproducibility was excellent for this criteria (K=0.8). In 2/3 of cases, the tumor was radiologically in contact with the cribriform plate (d2) and in 18% of cases a lysis of the cribriform plate was observed (d3). The tumor stayed at distance (d1) of the cribriform plate in less than 10% of cases, the best radiological sign being the persistance of air between the cribriform plate and the tumoral apex (air bubble sign, fig 2A). The reproducibility for the criteria distance (d1) and contact (d2) was respectively good (K=0.7) and excellent (K=0.8). The reproducibility for the criteria lysis with or without imprint were moderate (respectively 0.3 and 0.5).

3.2. Relationship with the ethmoidal labyrinth's roof

The concordance was excellent for this criteria (K=0.8). In more than 2/3 of cases, the tumor stayed at distance of the ethmoidal labyrinth's superior barrier, both of the vertical and horizontal portions (d1). In these cases, a triangle of air or retention, which were best identified on coronal T2 images, was observed under the ethmoidal roof. In most cases, the middle turbinate could be identified, limiting this triangle together with the ethmoid roof and the medial orbital wall (fig2B). Contact (d2, <10%) or lysis (d3+d4, <20%) of the ethmoid labyrinth's roof were encountered only in huge tumors. These cases were always associated with a lysis of the cribriform plate (p=0.01).

3.3. Relationship with the orbital wall

The concordance was excellent for this criteria **(**K=0.8), especially for the criteria distance (d1, K=0.8), lysis with or without imprint (d3a or d3b, K=0.8) and the subcriteria invasion of onodi cell (K=1, data not shown). Concordances were good (K=0.7) for tumoral contact with the orbital wall (d2), and the sub-criteria invasion of the internal angle of the orbit (data not shown). Most tumors (50%) were described as staying at distance of the orbital wall (d1), being separated of the orbital wall by the middle turbinate. The second more frequent presentation was suspicion of invasion of the orbit by the tumor (d3b). Invasion was suspected in two specific locations: either anteriorly where the tumor could invade the space between the ascending process of the maxilla and the eye ball (13%) (fig 2C), or posteriorly at the level of the orbital apex (18%) where the anatomical limits were difficult to follow because of the inconstant presence and variable pneumatization of Haller, Onodi, and anterior clinoid cells.

3.4. Relationship with the anterior sphenoid wall

The criteria anterior sphenoidal wall had the lowest concordance (K=0.5). The concordance was, however, excellent when tumors were at distance from the wall, with an aerial interface (K=0.9, data not shown). The sphenoid sinus was often invaded (40%), but the reproducibility for the two criteria lysis without penetration into the sphenoid sinus (d3a) and lysis with penetration in the sinus without involvement of the peripheral wall of the sinus (d3b) was low (respectively 0.5 and 0.2). The criteria involvement of the peripheral wall of the sphenoid sinus (d4a) was identified with an excellent reproducibility (K=0.8) : this situation was rare (1-3 cases). In fact, the most frequent presentation was tumoral contact with the anterior wall of the sphenoid, without lysis (47%).

3.5. Relationship with the nasal septum

There was no tumor at distance (d1) from the septum. In most cases (62%) the septum was pushed into the adjacent nasal fossa by the tumor (d3b, K=0.8), and invasion of the controlateral nasal fossa was suspected in 35% of cases with a good reproducibility (K=0.6).

Discussion

This study demonstrates that it is possible to describe and classify in a precise and reproducible way the relationships of nasal adenocarcinomas with the main anatomical barriers of the ethmoid bone.

Our work supports that the origin of woodworkers adenocarcinomas is in the olfactory cleft: in all cases, the tumor was in contact with the nasal septum and in the majority of cases showed contact with the cribriform plate, but stayed at distance from the ethmoidal roof and orbital wall, thus leading to the pathognomonic formation of a triangular air or retention signal (triangle sign) in the ethmoidal labyrinth squeezed under the anterior cranial base (fig 2B). The ethmoidal labyrinth's roof

Figure 1: Coronal CT-scan (bone window) with normal anatomy of the olfactory cleft.

The olfactory cleft (1) is a narrow cavity on each side of the nasal septum (2), which is limited:
- Laterally by the turbinate wall of the ethmoidal labyrinth (3), formed from top to bottom by the conchal plate of Mouret (4) (which is a continuous bony plate attached to the ethmoidal labyrinth's roof (5), and prolongs the lateral lamina (6) of the olfactory groove (7) under the level of the cribriform plate (8)) and below from front to back by the middle (9) then superior (then sometimes supreme) turbinates (which form a clearstory barrier between olfactory cleft and ethmoidal labyrinth)
- Medially by a portion of the nasal septum (2) corresponding to the perpendicular plate
- Superiorly, from front to back by the nasal bone, a portion of the frontal bone, the cribriform plate (8) and the ethmoidal process of the sphenoid bone.
- Posteriorly by the anterior wall of the sphenoid bone

The anterior and inferior walls are freely opening into the nasal fossa (10).

was actually reached only by advanced lesions showing simultaneous lysis of the cribriform plate. The origin of the tumor in the olfactory cleft has direct implications both in the evaluation of local extension and in the surgical approach to totally remove the tumor.

The anatomy of nasal fossa and paranasal sinuses is relatively complex. The description of the tumoral extension in these cavities is therefore hard to conceptualize and standardize. The method developed here, estimating the relationship between the tumor and the barrier, achieves an interesting

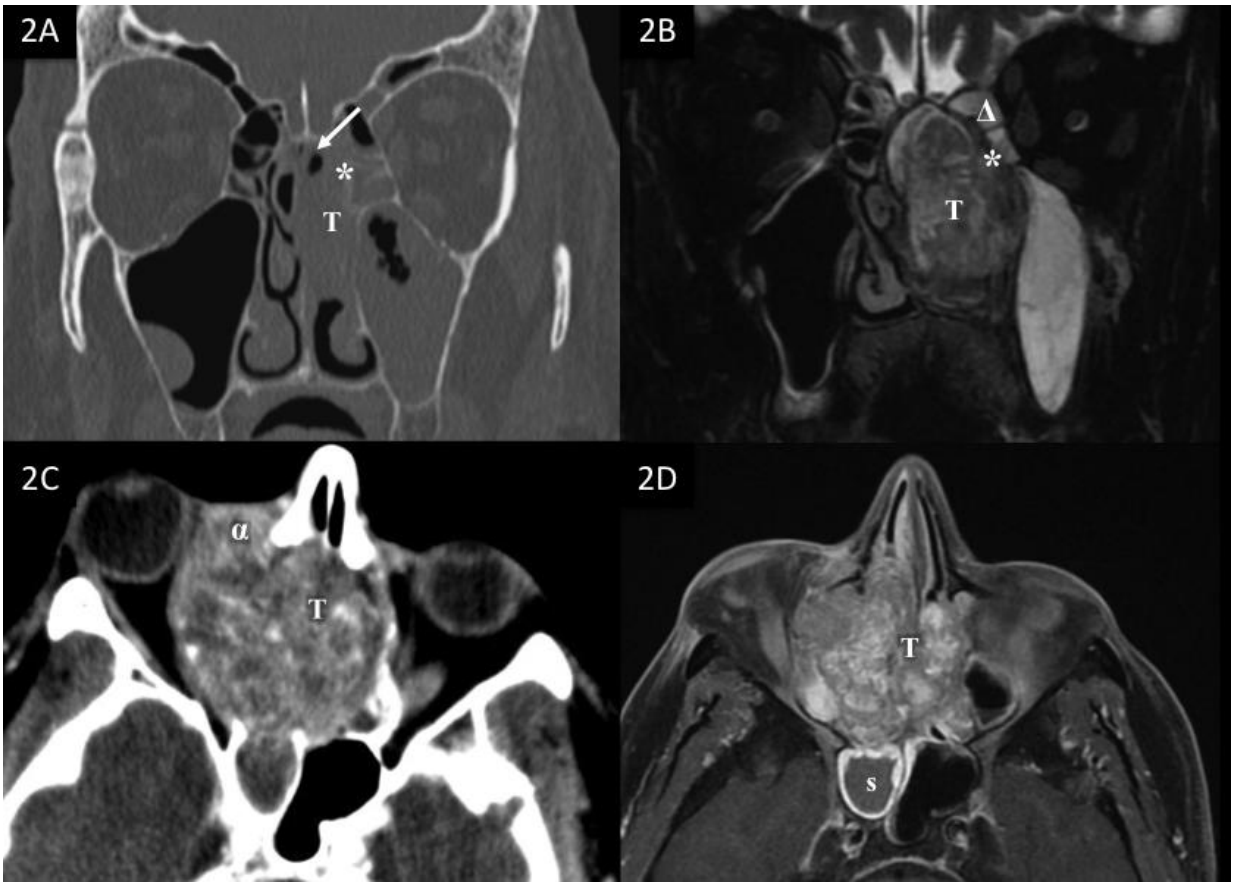

Figure 2: Illustrations of the classification (CP=cribriform plate, ER=ethmoidal labyrinth's roof, OW=orbital wall, SW=anterior sphenoid wall)

2A : Relationship between adenocarcinoma and cribriform plate: the "air bubble sign" (non enhanced coronal CT scan, bone tissue window)

The tumor (**T**) is located in the left olfactory cleft and nasal fossa. The turbinal wall is still visible (*****): the tumor is at distance from the orbital wall and from the ethmoidal roof (d1(OW), d1(ER)). There is an aerial interface between the tumor and the cribriform plate **(bubble sign, arrows).**

2B : Relationship between adenocarcinoma and ethmoidal labyrinth's roof ("triangular retention signal") (coronal T2-weighted MRI)

The tumor (**T**) has developed into the olfactory cleft and the nasal fossa. The turbinal wall is still visible (*****). The ethmoid is crushed laterally onto the orbital wall, under the ethmoidal labyrinth's roof. Retention of secretions and mucosal oedema inside the ethmoidal labyrinth leads to a triangular retention signal (**Δ**) suggesting that the tumor did not invade the ethmoidal labyrinth (d1(OW), d1(ER)). There is no contact with the left cribriform plate, on this slide (d1(CP))

2C: Relationship with the orbital wall (enhanced axial CT-scan: soft tissue window)

Bilateral tumor (**T**) centred on the right olfactory cleft. The tumor is invading the anterior internal angle of the orbit (**α**), between the ascending process of the maxilla and the eyeball, an area of difficult access for endoscopic endonasal surgery, which need to be approached externally.

2D: Relationship with the anterior sphenoid wall (axial T1-weighted MRI, fat-sat, Gadolinium)

The orbital wall is destroyed by the tumor (**T**) but the periosteum is pushed in a homogeneous manner, so that it is probably not invaded. While the sphenoid sinus appears invaded on CT-scan (fig 2C, d4a(SW)), the MRI clearly evidences the inflammatory sphenoid mucosae with a sphenoid sinus full of retention (**s**) (d3a(SW)).

reproducibility in the interpretation of radiological tumoral extension and a leads to a description matching the expectations of surgeons and even radiotherapists.

Indeed, the distance to the organs at risk is indeed an important element of decision both for the surgeon and the radiation therapist. A tumor remaining at distance of the anatomical barrier (d1) will be resected without major difficulty and probably with safe margins . As soon as the lesion comes into contact with the barrier (d2), this proximity may end up with difficult resection during surgery. The risk of incomplete excision increases with tumor crossing the studied barrier (d3). Finally, in "d4 tumors", surgery becomes heavy, with sometimes difficult decision between endoscopic endonasal craniofacial resection and external approach combining lateral rhinotomy and transcranial approaches. In these cases, radiotherapy will also be limited by the proximity of organs at risk (eye, optic nerve, chiasma...).

To our knowledge, reproducibility has never been tested for the different published classifications of extension of sino-nasal tumors. The reproducibilities of classifications used in practice in radiology usually show kappa values between 0.4 and 0.8(12)-(13) and sometimes even inferior to 0.4(14)-(15)-(16). In general, the best concordances are observed for classifications with few criteria of judgment, few stages or geometric measurement(10). Our method of radiological assessment of the tumoral extension is highly reproducible despite the numerous criteria used. But , although the teams were made up of trained senior, the agreement is not total between responses, which highlights the difficulties sometimes encountered in the therapeutic decision.

The main difficulty encountered was to determine if the sphenoid sinus was involved or not by the tumor. The complex shape of its anterior wall and the presence of the ostium might simulate lysis of the anterior wall. Because of the site of tumoral onset, the sphenoid sinus is often subject to inflammation and/or retention. This may simulate tumoral invasion, that only MRI can eliminate, if appropriate sequences are available. In T2-weighted sequences, the tumoral signal is lower than the high signal of inflammatory tissues or retention(17). In some difficult cases of tumoral inflammatory changes or chronic retention with high proteic content, the injection of Gadolinium can be discriminant in comparison with non-injected sequences (in those cases, retention appears spontaneously hyperintense on T1 sequences, without enhancement after injection, fig2D)(18). Though, a simple tumoral protrusion in the sphenoid sinus is not a surgical challenge in endoscopic endonasal approach. The real surgical difficulties start with lesions for which lysis of the peripheral walls of the sphenoid sinus is suspected(19), which are rare situations (1-3 cases, <10%) and for which radiological assessment seems easy (K=0.8).

The presence of air between the tumor and one barrier ("air bubble sign", fig 2A) is a reliable radiological sign to consider that the tumor stays at safe distance from the barrier (K=0.8). The disappearance of this sign may be the consequence of juxta-lesional inflammation and/or retention of secretions. It increases the difficulty to interpret the relationship with the surrounding barriers in the way that extension might be overestimated. The same difficulty is encountered for deciding between integrity and lysis of a bony wall when the tumor is in contact with it. Indeed, the radiological contrast is not sufficient at the interface bone/tumor, especially at the level of the cribriform plate (K=0.3), because it is thin and naturally perforated bone. Classically, the integrity of the cribriform plate is better studied with coronal reconstructions of the CT-scan, but apparent normality does not eliminate a peri-nervous diffusion or a small lysis allowing intracranial extension(20). MRI is therefore mandatory in these situations: the absence of intracranial extension is easy to assess on coronal T2 sequences, since the CSF hypersignal enables a good visualisation of the olfactory bulb and dura mater (K=0.7).

Due to the site of onset of these tumors, the integrity of the ethmoidal roof is generally well preserved in early stage adenocarcinomas. Though, the presence of inflammation or retention in ethmoidal cells may be misleading: in these cases, the association of CT-scan and MRI is helpful. In advanced stages, the lysis usually begins on the medial side, beside the olfactory groove. As the ethmoidal roof is thicker than the olfactory cleft, lysis is better identified (K=0.7).

Assessing the invasion of the adjacent organ may be challenging, so that MRI is usually necessary. Because of its protection by the middle turbinate, the invasion of the orbit generally begins anteriorly (behind the frontal process of the maxillar, at the level of the lamina papyracea) or posteriorly (orbital apex). Once the bone destroyed, the periorbita acts like a barrier to tumor spread: a

regular displacement of the orbital content is usually associated with the respect of the orbital content, while a nodular aspect is highly suspect, even if this sign is not completely specific (7). The disparition of the orbital fat - because of its invasion - is well seen on MRI (T1 weighted coronal sequences), as an enlargement, abnormal signal or abnormal enhancement of the extra-ocular muscles (T1 with gadolinium and T2 weighted coronal sequences), which are very specific signs of orbital invasion (7). This differentiation was not really problematic in our study (K=0.8). As for the dura mater, a thickening of more than 5 mm in length, with nodular or irregular aspect must be considered highly suspect, especially if there is association with thickening of the leptomeninges (8). Assessing the invasion of the cerebral cortex may be difficult when the tumor already reaches the dura mater (K=0.5). As adenocarcinomas have a low ability to invade adjacent tissues, it seems that as long as the cortex remains visible in MRI (T1 or T2), the risk of cerebral involvement is low. The cerebral invasion may be suspected when enhancement of the brain cortex is present, especially with adjacent oedematous reaction in the parenchyma (9), better seen on MRI (fig 2E).

The association of CT-scan and MRI is therefore mandatory, even if there is no suspicion of intracranial invasion(20). Clement and Lund reported a radiohistologic correlation of 85.2% with CT-scan alone, 94.2% with MRI alone and 98.5% with both exams(21)-(22). We recommend that 1/ MRI should at least include the following 6 series: axial-T1, axial-T2, coronal-T2, and axial, coronal and sagittal T1+Gadolinium sequences and 2/ the CT-scan should always include an axial bone-window millimetre series, thus permitting coronal reconstructions and tissular axial series. Simultaneously, the CT-scan should check for regional extension and pulmonary or hepatic metastasis.

Conclusion:

This study shows that it may be possible to stage the local extension of nasal adenocarcinomas according to their relationship with the main barriers of the olfactory-ethmoidal cavities, thus leading to rationalized therapeutic decision

Abbreviations:

ENT	otorhinolaryngologist
ADC	adenocarcinoma
CSF	cerebrospinal fluid
CT	computed tomography
MRI	Magnetic resonance imaging
CP	cribriform plate
ER	ethmoidal labyrinth's roof
OW	orbital wall
SW	anterior sphenoid wall

References

1. Jankowski R, Georgel T, Vignaud JM, Hemmaoui B, Toussaint B, Graff P, et al. Endoscopic surgery reveals that woodworkers' adenocarcinomas originate in the olfactory cleft. Rhinology. 2007 Dec;45(4):308-14.
2. Georgel T, Jankowski R, Henrot P, Baumann C, Kacha S, Grignon B, et al. CT assessment of woodworkers' nasal adenocarcinomas confirms the origin in the olfactory cleft. AJNR Am J Neuroradiol. 2009 Aug;30(7):1440-4. DOI: 10.3174/ajnr.A1648.
3. Vergez S, du Mayne MD, Coste A, Gallet P, Jankowski R, Dufour X, et al. Multicenter study to assess endoscopic resection of 159 sinonasal adenocarcinomas. Ann Surg Oncol. 2014 Apr;21(4):1384-90. DOI: 10.1245/s10434-013-3385-8.
4. Grosjean R, Gallet P, Baumann C, Jankowski R. Transfacial versus endoscopic approach in the treatment of woodworker's nasal adenocarcinomas. Head Neck. 2015 Mar;37(3):347-56. DOI: 10.1002/hed.23601.
5. Choussy O, Ferron C, Védrine PO, Toussaint B, Liétin B, Marandas P, et al. Adenocarcinoma of Ethmoid: a GETTEC retrospective multicenter study of 418 cases. Laryngoscope. 2008 Mar;118(3):437-43. DOI: 10.1097/MLG.0b013e31815b48e3.
6. Bodino C, Jankowski R, Grignon B, Jimenez-Chobillon A, Braun M. Surgical anatomy of the turbinal wall of the ethmoidal labyrinth. Rhinology. 2004 Jun;42(2):73-80.
7. Eisen MD, Yousem DM, Loevner LA, Thaler ER, Bilker WB, Goldberg AN. Preoperative imaging to predict orbital invasion by tumor. Head Neck. 2000 Aug;22(5):456-62.
8. Eisen MD, Yousem DM, Montone KT, Kotapka MJ, Bigelow DC, Bilker WB, et al. Use of preoperative MR to predict dural, perineural, and venous sinus invasion of skull base tumors.

AJNR Am J Neuroradiol. 1996 Nov-Dec;17(10):1937-45.
9. Kraus DH, Lanzieri CF, Wanamaker JR, Little JR, Lavertu P. Complementary use of computed tomography and magnetic resonance imaging in assessing skull base lesions. Laryngoscope. 1992 Jun;102(6):623-9.
10. Sim J, Wright CC. The kappa statistic in reliability studies: use, interpretation, and sample size requirements. Phys Ther. 2005 Mar;85(3):257-68.
11. Landis JR, Koch GG. The measurement of observer agreement for categorical data. Biometrics. 1977 Mar;33(1):159-74.
12. Beaulé PE, Dorey FJ, Matta JM. Letournel classification for acetabular fractures. Assessment of interobserver and intraobserver reliability. J Bone Joint Surg Am. 2003 Sep;85-A(9):1704-9.
13. Bernstein J, Adler LM, Blank JE, Dalsey RM, Williams GR, Iannotti JP. Evaluation of the Neer system of classification of proximal humeral fractures with computerized tomographic scans and plain radiographs. J Bone Joint Surg Am. 1996 Sep;78(9):1371-5.
14. Martin JS, Marsh JL, Bonar SK, DeCoster TA, Found EM, Brandser EA. Assessment of the AO/ASIF fracture classification for the distal tibia. J Orthop Trauma. 1997 Oct;11(7):477-83.
15. Doornberg J, Lindenhovius A, Kloen P, van Dijk CN, Zurakowski D, Ring D. Two and three-dimensional computed tomography for the classification and management of distal humeral fractures. Evaluation of reliability and diagnostic accuracy. J Bone Joint Surg Am. 2006 Aug;88(8):1795-801.
16. Koo H, Leveridge M, Thompson C, Zdero R, Bhandari M, Kreder HJ, et al. Interobserver reliability of the young-burgess and tile classification systems for fractures of the pelvic ring. J Orthop Trauma. 2008 Jul;22(6):379-84. DOI: 10.1097/BOT.0b013e31817440cf.
17. Som PM, Shapiro MD, Biller HF, Sasaki C, Lawson W. Sinonasal tumors and inflammatory tissues: differentiation with MR imaging. Radiology. 1988 Jun;167(3):803-8.
18. Lanzieri CF, Shah M, Krauss D, Lavertu P. Use of gadolinium-enhanced MR imaging for differentiating mucoceles from neoplasms in the paranasal sinuses. Radiology. 1991 Feb;178(2):425-8.
19. Cantù G, Solero CL, Miceli R, Mariani L, Mattavelli F, Squadrelli-Saraceno M, et al. Which classification for ethmoid malignant tumors involving the anterior skull base? Head Neck. 2005 Mar;27(3):224-31.
20. Ferrié JC, Martin-Duverneuil N, Dufour X, Klossek JM. [Role of imaging in the pre-treatment assessment and post-treatment follow-up of sinonasal malignancies]. J Radiol. 2008 Jul-Aug;89(7-8 Pt 2):984-97.
21. Clement O, Serrano E, Pessey JJ. [Adenocarcinomas of the ethmoid sinuses. Diagnosis and treatment, a propos of 43 cases]. Les cahiers d'ORL 1998;8:414-419. http://www.rforl.com/PDF/UK0508903.pdf
22. Lund VJ, Howard DJ, Lloyd GA, Cheesman AD. Magnetic resonance imaging of paranasal sinus tumors for craniofacial resection. Head Neck. 1989 May-Jun;11(3):279-83.